Available online at www.sciencedirect.com
SCIENCE DIRECT®
International Journal of Heat and Mass Transfer 48 (2005) 1727–1738
International Journal of HEAT and MASS TRANSFER
www.elsevier.com/locate/ijhmt

Heat transfer characteristics of an array of impinging pre-mixed slot flame jets

L.C. Kwok, C.W. Leung *, C.S. Cheung

Department of Mechanical Engineering, The Hong Kong Polytechnic University, Hung Hom, Kowloon, Hong Kong, PR China

Received 22 March 2004; received in revised form 24 November 2004
Available online 29 January 2005

Abstract

An experimental study was carried out to investigate the shape and the heat transfer characteristics of an array of three laminar pre-mixed butane/air slot flame jets impinging upwards normally on a horizontal water-cooled flat plate. The effects of jet-to-jet spacing and nozzle-to-plate distance were examined at the Reynolds number (Re) of 1000 and the equivalence ratio (ϕ) of unity. Comparisons of the heat transfer characteristics between single and multiple slot flame jets, as well as multiple slot and round jets, were made. The between-jet interference decreased with increasing jet-to-jet spacing (s/d_e) and nozzle-to-plate distance (H/d_e). Strong interference was obtained at $s/d_e = 1$ and $H/d_e = 2$, at which the central jet was suppressed while the side jets were deflected towards their free sides. In addition, there was no minimum heat flux found in the inter-jet interacting zone, instead, a peak heat flux was obtained. Thermal performance was reduced when H/d_e became smaller than the length of the conical luminous reaction zone of the flame. A maximum average heat flux occurred at the moderate jet-to-jet spacing of $s/d_e = 2.5$ at $Re = 1000$, $\phi = 1$ and $H/d_e = 2$. The resultant heat flux distribution of the central jet of a multiple slot jets system was higher than that of a single slot jet when the jet-to-jet spacing was small, but this advantage in thermal performance diminished when the jet-to-jet spacing was increased. Besides, the area-averaged heat flux of the multiple slot flame jets was higher than that of the multiple round flame jets arranged at the same geometric configuration.

Keywords: Impingement heat transfer; Multiple slot flame jets; Pre-mixed butane/air combustion

1. Introduction

Impinging burners are widely used in rapid-heating furnaces to save energy and time, since the turbulent forced convection obtained by impinging the flames on the object can enhance heat transfer significantly [1]. Multiple impinging flame jets are normally adopted for both industrial and domestic heating applications, as jets arranged in an array can help to enhance the heat transfer for heating up a large surface area and to avoid the occurrence of local hot spots. However, information on impinging multiple flame jet systems is very rare, especially about slot jets, despite their popularity in application. With the aim of providing fundamental understanding of the flame shape and heat transfer characteristics of the multiple impinging slot flame jets, the present work was performed to study the thermal performance of a row of three premixed butane/air laminar slot flame jets.

* Corresponding author. Tel.: +852 2766 6651; fax: +852 2365 4703.
E-mail address: mmcwl@polyu.edu.hk (C.W. Leung).

0017-9310/$ - see front matter © 2005 Elsevier Ltd. All rights reserved.
doi:10.1016/j.ijheatmasstransfer.2004.11.014

Nomenclature

d	nozzle exit diameter (m)	u	velocity of butane/air mixture (m/s)
d_e	effective nozzle exit diameter (m) ($d_e = (4wl/\pi)^{1/2}$)	v	flame velocity near the stagnation point (m/s)
H	distance between the nozzle and the impingement plate (m)	w	rectangular nozzle width (m)
l	rectangular nozzle length (m)	x	displacement on impingement plate along direction of the slot length (m)
$\dot{q}$	local heat flux density (W/m^2)	y	displacement on impingement plate along direction of the slot width (m)
$\bar{q}$	average heat flux density (W/m^2)	ν	kinematic viscosity (m^2/s)
Re	effective nozzle exit diameter based Reynolds number ($=ud_e/\nu$)	ϕ	equivalence ratio (=(stoichiometric air/fuel volume ratio)/(actual air/fuel volume ratio))
s	distance between the centers of the two nozzles (m)		

Since there has been very little information available on multiple flame jets, studies of multiple isothermal air jets [2–13] were therefore found useful in providing foundation for the present investigation. Koopman and Sparrow [2] studied a row of impinging air jets and concluded that a higher local heat transfer coefficient was obtained midway between adjacent jets owing to the collision of their spreading flows. This collision effect became obvious at high jet Reynolds numbers, small jet-to-jet spacing and small jet-to-plate distance. Huber and Viskanta [8] and Saad et al. [9,10] studied the effects of jet-to-jet spacing and nozzle-to-plate distance on the thermal performance of the multiple isothermal air jets. The jet-to-jet spacing was suggested to affect the convective heat transfer coefficient significantly. The studies were conducted by varying the influence of the adjacent jet interference and fraction of the impingement target surface covered by the wall jet.

Barata et al. [11,12] visualized the flow impinging downwards to a horizontal surface and found that the fountain upwash flow formed by collision of the radial wall jets was deflected by the crossflow. Seyedein et al. [13] studied the laminar flow and heat transfer characteristics of the multiple impinging slot air jets by numerical simulation. A disadvantage of impinging jets was suggested to be the highly non-uniform heat transfer distribution over the impingement surface with a peak Nusselt number occurring in the wall jet region.

Because of the very complicated flow field of the multiple impinging jets, presentation of the results in the form of average heat transfer coefficient is usually preferable. Martin [5] applied the technique of relative nozzle area to analyze and compare the average heat transfer coefficients of single and multiple impinging hot air jets, which were emitting from both round and slot nozzles. For an array of impinging round air jets, the jet-to-jet spacing corresponding to a maximum average heat transfer coefficient was found to be $7d$ at $H/d = 5.4$.

Compared with the number of investigations on heat transfer characteristics of multiple impinging air jets, there are almost no studies with multiple impinging flame jets. Most of the previous investigations of impinging flame jets are concerned with the single round jet [1,14–19]. However, heat transfer characteristics of the multiple flame jet system are rather different from those of the single jet due to the existence of jet-to-jet interactions, which cannot be identified from the single jet system [8,20].

A good understanding of the interaction between adjacent flame jets, both before and after the impingement, is yet uncertain. Most of the available information on multiple impinging flame jets is related to the radial jet reattachment flames [21,22]. Wu et al. [22] studied a row of three radial jet reattachment flames and concluded that high pressure could be observed in the interaction region at the midpoint between the two neighboring nozzles. High surface heat fluxes were obtained at a moderately interactive configuration of a jet-to-jet spacing of $S/R_0 = 8$. Among the very few investigations of the multiple impinging flame jet system, Dong [19] studied an array of two round flame jets and triple in-line round flame jets. A significant interference was found in the flame between the jets, especially when both the jet-to-jet spacing and nozzle-to-plate distance were small. The between-jet interference reduced the heat transfer in the interacting zone. An optimal heat transfer occurred when both the jet-to-jet spacing and the nozzle-to-plate spacing were set at a moderate value of 5. Comparison between the single and multiple impinging flame jets was not made, such that the difference in their thermal characteristics was not fully identified.

Very little work has been done for single or multiple impinging slot flame jets [23–25]. From the few reports in the literature, it has been pointed out that interaction between adjacent jets could affect the heat transfer of the flame jets significantly, but the extent of such interaction

is not yet known. The present study is therefore conducted to solve these uncertainties.

A row of three flame jets was chosen because it provided the most basic arrangements, which were found in an array consisting of a large number of jets. The configuration of a central jet surrounded by two side jets is similar to the situation of any jet in a jet array. The central jet experiences interference from its two neighboring jets and the effect can be used to characterize the behavior of any jet in a large jet array except that at the free end, which is affected by its neighboring jet from one side only. Experimental study was conducted to observe the flame shape and local heat flux distribution along the plate surface impinged by an array of slot flame jets. Focus was placed to the interaction between the two adjacent jets and its effect on the heat flux distribution on the impingement plate. Effects of the most important geometric parameters of the multiple flame jet system, i.e., the jet-to-jet spacing and nozzle-to-plate distance, on its flame shape and heat transfer coefficient at the jet/plate interface have been examined.

2. Experimental setup and method

The flame impingement system of the present study is shown schematically in Fig. 1(a) and (b). The nozzles and the flame holder were attached to a three-dimensional

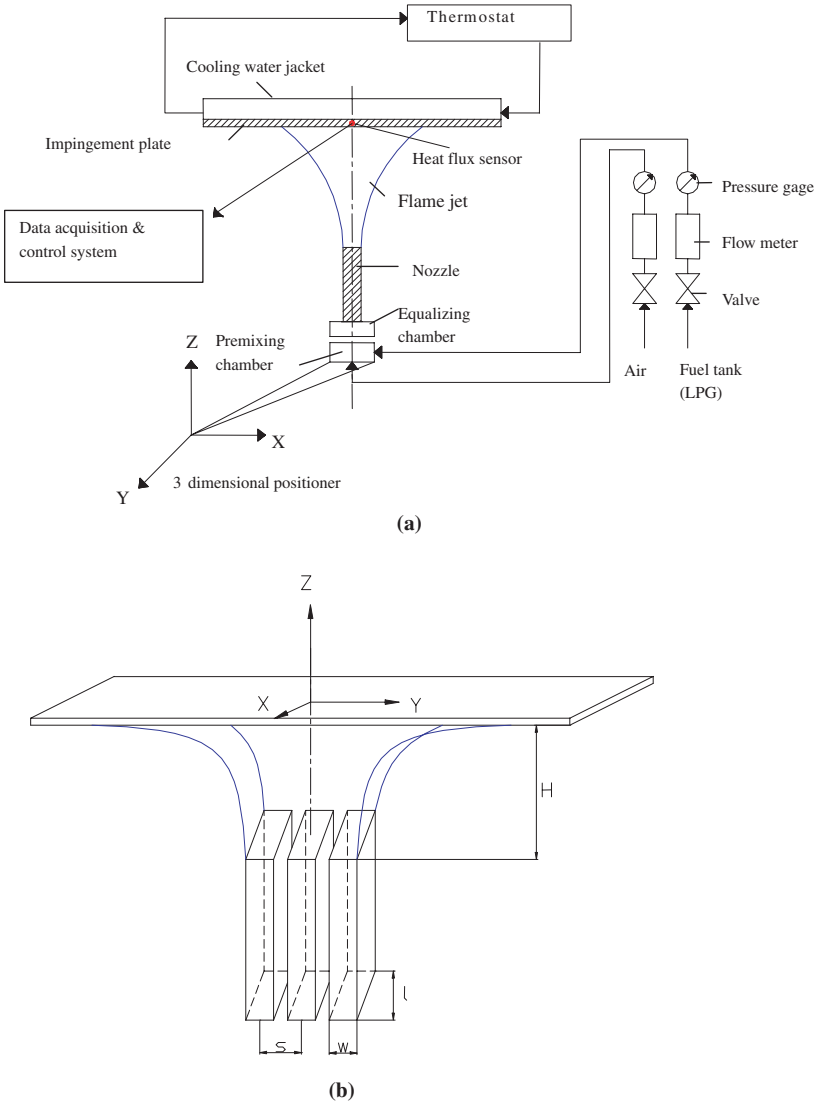

Fig. 1. Experimental setup. (a) Schematic and (b) impingement flame jets system.

positioner such that they could be located at a desired position relative to the impingement surface. The flame holder consisted of three identical slot copper ducts; each had an inner dimension of 13.4×4.3 mm^2 (equivalent to an effective nozzle exit diameter, $d_e = 8.56$ mm) and a length of 300 mm. There were three jet-to-jet spacings, $s/d_e = 1$, 2 and 3, used to represent the small, moderate and large jet-to-jet spacings.

Butane gas and compressed air were metered with rotameters and pre-mixed to generate the flames. The rotameters had been well calibrated with a soap-bubble meter. In order to prevent the non-uniform air/fuel flows and misdistribution caused by interaction between the three jets, the flow rate in each of these three nozzles was controlled and measured individually. It was to ensure that each nozzle could be operated under identical and stable flow condition. The three flame jets impinged vertically upward onto a water-cooled copper impingement plate having a surface area of 500×500 mm^2 and a thickness of 8 mm. The cooling water was kept at a temperature of 38 °C by a refrigerator to eliminate the condensation of water vapor on the impingement plate surface [17,18].

A heat flux transducer having an effective sensing area of 6 mm^2 was installed at the center of the flame-side surface of the impingement plate to measure the local heat flux from the flame to the plate. By moving the three-dimensional positioner horizontally in the x–y plane, the local heat flux of a point on the impingement plate relative to the stagnation point could be measured, such that the heat flux distributions in the x- and y-directions of the impingement plate were obtained. The three-dimensional positioner could also be fixed at different locations along the z-direction to achieve various nozzle-to-impingement-plate distance, such that $H/d_e = 2$, 3, 4 and 6 in the present investigation. The approach had been applied satisfactorily in the Authors' previous studies [26,27]. A data acquisition system was used to record the heat flux data. Every reported data is the average value of the data obtained consecutively in two minutes at a rate of 500 samples per second. A digital camera of 5,000,000 pixels was used to record the flame shapes.

3. Reliability of experimental results

An uncertainty analysis has been carried out according to the method proposed by Kline and McClintock [28]. Using a 95% confidence level, the maximum and minimum uncertainties for the presented local heat flux are 12.8% and 3.2%, respectively. The thermal radiation was assumed negligible because of the non-luminous radiation resulting from burning butane with air, and the relatively low surface emissivity of the impingement surface (around 0.2) [15,25,29]. Besides, the highly transient nature of the flame jets had been highly alerted during the entire study. A data acquisitition system was used to record the heat flux values after the system became stable and steady. Use of the sampling rate of 500 samples per second for the duration of 120 s in recording every reported data is to ensure repeatability.

4. Results and discussion

Experiments were conducted to study the influence of s/d_e and H/d_e on the flame shape and heat transfer characteristics of a row of three laminar impinging slot flame jets. Attention was focused on the stoichiometric combustion ($\phi = 1$) and laminar flow condition ($Re = 1000$). The non-dimensional jet-to-jet spacing, s/d_e, was varied from 1, 2 and 3 to represent the small, moderate and large spacings, whereas the non-dimensional nozzle-to-plate distance, H/d_e, was set at a value between 2 and 6 to ensure the inclusion of the inner luminous cone of the flame.

4.1. Flame appearance

Photographs of the triple impinging slot flame jets at the small, moderate, and large jet-to-jet spacings, i.e., $s/d_e = 1$, 2, and 3, under two nozzle-to-plate distances (H/d_e) of 2 and 4, are shown in Fig. 2(a) and (b). Flame shapes of the single impinging slot flame jet were also provided for the purpose of comparison. All photographs were taken along the direction of the slot width, with the width of the jet placed normal to the camera.

It could be observed from the photographs that both the single flame jet and each of the multiple flame jets consisted of an inner zone of unburned gases, a thin blue layer of conical luminous reaction zone and a light blue outer layer of burned gases. In the multiple flame jet system, each of the triple flame jets was basically having the similar shape as the single flame jet. There was certain distortion in each flame due to the interaction between the adjacent flame jets, and the level of interaction and hence distortion was dependent directly on the jet-to-jet spacing as well as the nozzle-to-plate distance.

In Fig. 2(a), at $H/d_e = 2$ and $s/d_e = 1$, outer layers of the adjacent flame jets were found to merge together. The small spacing between the adjacent flame jets confined the flow of the central flame jet and pushed the side flame jets outwards. At the same time, the central jet was suppressed by the side jets so that its inner reaction zone became slightly shorter. It might be due to two types of interaction occurring at the small jet-to-jet spacing and nozzle-to-plate distance: interference between adjacent flame jets before impinging on the surface and collision of the wall jets associated with the adjacent impinged jets [2].

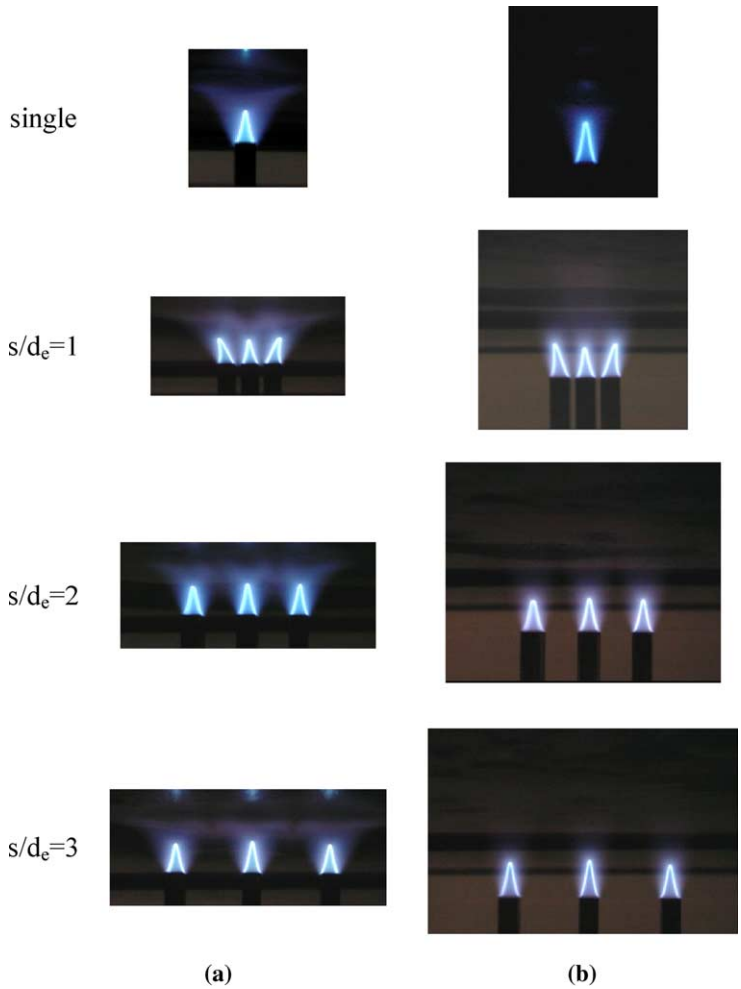

Fig. 2. Photographs of the triple and single impinging slot flame jets. (a) $Re = 1000$; $\phi = 1$; $H/d_e = 2$ and (b) $Re = 1000$; $\phi = 1$; $H/d_e = 4$.

At $s/d_e = 1$, the outer layers of adjacent jets merged and the side jets were pushed to deflect outwards. At $s/d_e = 2$ and $s/d_e = 3$, the outer layers impinged against each other and were deflected downwards away from the impingement plate after impinging with each other at the mid-point between them to form a "W-shaped" outer flame layer. However, such flame feature was not observed at higher H/d_e and became more obvious at the smallest H/d_e ratio of 2 and the largest s/d_e ratio of 3. At $s/d_e = 3$, the larger spacing between the adjacent flame jets allowed their outer layers to spread into the interacting zone and flow downwards upon impingement with each other, resulting in the "W-shaped" outer flame layer [30].

A stronger interference between the adjacent flame jets was obtained at smaller nozzle-to-plate distance. When H/d_e was increased to 4 as shown in Fig. 2(b), this effect was less obvious. At $s/d_e = 2$, the outer layers of adjacent jets merged only along the impingement plate to meet each other at their mid-point and there was little distortion occurred at the side jets. At $s/d_e = 3$, the three jets appeared to be three isolated single flame jets. There was no "W-shaped" outer flame layer observed at $H/d_e = 4$, indicating a rather weak between-jet interference.

The between-jet interference occurred at different jet-to-jet spacings as observed from the flame appearance could be supplemented by the variation of the local pressure on the impingement surface, which was obtained in the Authors' previous work [31]. Conclusively, it can be assumed that the chance to obtain a diffusion flame at the present equivalence ratio ($\phi = 1$) is quite negligible.

4.2. Local heat flux distribution

Fig. 3(a) and (b) show the effect on the heat transfer performance of the jet-to-jet spacing and the nozzle-to-plate distance, via the local heat flux contours of a single slot flame jet and those of the triple slot flame jets with

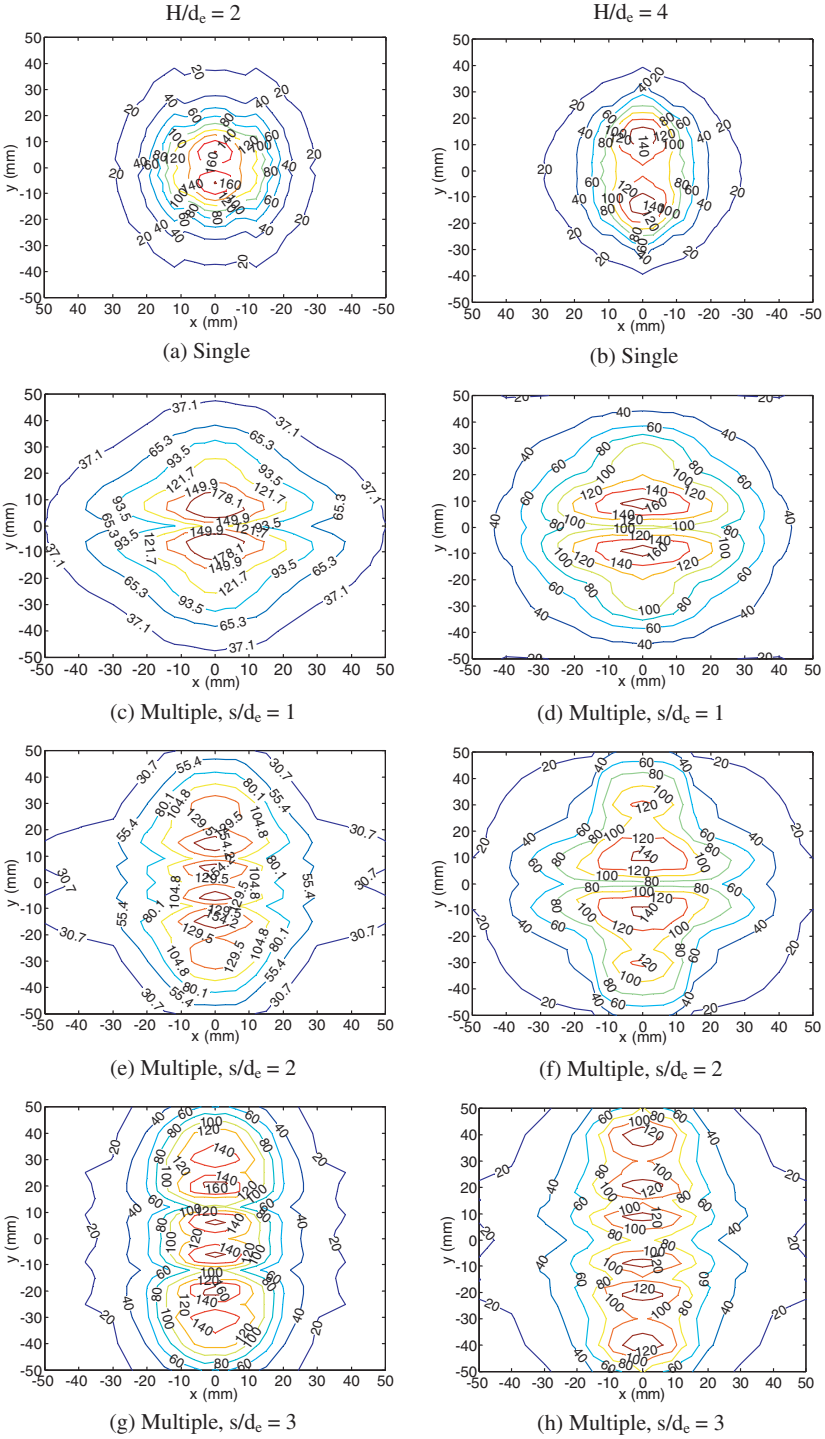

Fig. 3. Heat flux contours of single and triple impinging slot flame jets (Re = 1000; ϕ = 1).

s/d_e = 1, 2 and 3, at H/d_e = 2 and 4, respectively. A comparison of heat flux distribution along the impinging plate between the single and multiple slot flame jets has been made. It was found that the heat flux distribution of the single flame jet decreased rapidly in the radial direction, whereas that of the multiple flame jets was higher in the wall-jet region and decreased relatively slowly in the radial direction due to the additional

impingements. The multiple jet system showed the advantage in producing more uniform local heat flux distribution on the impingement plate than its counterpart. The other advantages in using multiple jets would be discussed in the following section, ''area-averaged heat flux distribution''.

The jet-to-jet interference, which was the special feature of the multiple flame jets, usually led to a lower heat transfer in the interacting zone because the between-jet action forced the flow to move downwards and detach from the impingement surface in this zone. At the small jet-to-jet spacing of $s/d_e = 1$, the flame jets interacted with each other such that the central jet was suppressed while the side jets were forced to deflect outwards as described previously. There was more outward flow obtained along the x-direction at the smaller jet-to-jet spacing when comparing with that occurring with the single jet. The behavior of three isolated single flame jets was clearly observed at the highest s/d_e ratio of 3, and each of the triple flame jets had sufficient spacing to develop freely and very little effect of the jet-to-jet interference could be observed.

When the nozzle-to-plate distance was increased to 4, lower local heat flux was found when compared with that obtained at the smaller H/d_e ratio of 2. The larger distance between the reaction zone of the flame and the impingement plate caused a reduction in the thermal performance of the flame jets system due to the entrainment of excessive surrounding air. In addition, the increased nozzle-to-plate spacing led to a lesser outward flow along the x-direction of the slot nozzle than that obtained at the smaller H/d_e ratios due to the reduced between-jet interference.

In order to explore more information about the effects of s/d_e and H/d_e on the heat transfer performance of an array of impinging slot flame jets, the variations of local heat flux with these parameters are discussed in the following sections.

4.3. Effect of jet-to-jet spacing (s/d_e)

Fig. 4(a) shows the local heat flux distributions on the impingement plate along the width direction of the single and triple slot flame jets with $s/d_e = 1$, 1.5, 2, 2.5 and 3, respectively, when $H/d_e = 2$. The corresponding flame shapes of the single and triple jets with $s/d_e = 1$, 2 and 3 are shown in Fig. 2(a) as reference. In Fig. 4(a), the line at $y = 0$ is the centerline of the central jet, while those at $y = 8.6$ mm, 12.9 mm, 17.2 mm, 21.5 mm and 25.8 mm correspond to the centerline of the side jet for $s/d_e = 1$, 1.5, 2, 2.5 and 3, respectively, as shown by the dotted line in the figure. Because of symmetry, another half of the figure (from 0 to 40 mm) was assumed to be the mirror image.

The single flame jet had a relatively low heat flux at the stagnation point, which was increased to a maximum value at $y = 7$ mm and then reduced steadily for further increase in the radial distance. For the triple flame jets, the highest heat flux at the impingement plate was obtained at the smallest s/d_e of 1. As s/d_e was increased, there was more than one maximum heat flux obtained on the impingement plate with similar value, which was also close to the peak heat flux of a single slot flame jet operating under the same condition. It shows that the inter-jet interference became stronger when the jet-to-jet spacing was small, and such effect was particularly obvious at the small nozzle-to-plate distance. As a result, the heat transfer would be much enhanced.

In all cases, the heat flux was low at the center of the central jet, indicating the existence of a cooler central core in this region. For $s/d_e = 1$, the heat flux increased to a peak value at $y = 7.5$ mm, which was near to the center of the side jet, and then decreased monotonically along the plate. For $s/d_e = 2$, there were three peak values and three minimum values observed. The first peak value occurred at $y = 6$ mm, which was near to the center of the central jet. The second peak value was occurred at $y = 15$ mm, which was on the interacting side and near to the center of the side jet. The third peak value occurred at $y = 30$ mm, which was on the non-interacting side of the side jet. Hence, there were two peaks in the interacting zone between the central jet and the side jet, and one peak on the non-interacting side of the side jet. The first minimum value occurred at the center of the central jet. The second minimum value occurred at $y = 10$ mm, which was in the interacting zone between the central and side jets. The third minimum value occurred at $y = 22$ mm, which was on the non-interacting side of the side jet. At $s/d_e = 3$, three peak values again occurred at the similar positions. There were also three minimum values. The first and third minimum values were located at the centers of the central and side jets, while the second minimum value was located between them.

From Fig. 2(a), at $s/d_e = 3$, the three jets acted almost independently. Hence, the minimum values were found at the center of the adjacent jets, indicating that the heat flux of the side jet was not influenced by the central jet, or vice versa. On the other hand, at $s/d_e = 1$, the cooler central core of the side jet disappeared due to the inter-jet interference from the central jet, while that of the central jet remained. At $s/d_e = 2$, location of the cooler central core of the side jet was forced to the non-interacting side, indicating that there was still interaction between the adjacent jets but it was much weaker when compared with that at $s/d_e = 1$. According to Fig. 4, it shows that the maximum heat flux was obtained at the smallest s/d_e ratio of 1 at $y = 7.5$ mm. For the other s/d_e ratios of 1.5, 2, 2.5 and 3, their measured highest heat fluxes were close to each other but lower than that of $s/d_e = 1$. At $s/d_e = 1$, the between-jet interference enhanced the heat transfer in this region and such thermal performance enhancement decreased as s/d_e was increased.

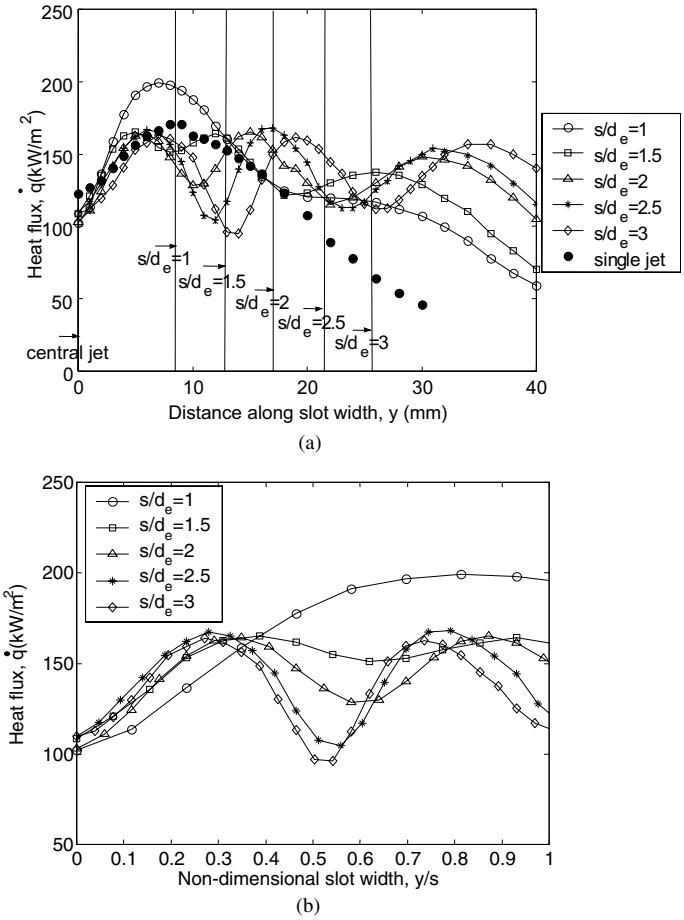

Fig. 4. Heat flux distribution at different jet-to-jet spacings (Re = 1000; ϕ = 1; H/d_e = 2). (a) Along slot width and (b) along non-dimensional slot width.

Fig. 4(a) was rearranged into Fig. 4(b) to show the local heat fluxes of the triple slot flame jets for different s/d_e ratios against the non-dimensional distance (y/s) along the impingement plate, which enabled the change of heat flux in the between-jet region to be observed clearly. At s/d_e = 1, the minimum heat flux occurred at the center of the central jet (y/s = 0). The heat flux increased to a maximum value at y/s = 0.8, but not at y/s = 0.5 (the mid-point of the two flame jets) due to the outward deflection of the side jets as shown in Fig. 2(a).

When the jet-to-jet spacing was increased to exceed 1, two distinctive heat flux peaks were obtained with a minimum heat flux located between the two peaks. The minimum heat flux occurred at y/s = 0.62, 0.58, 0.55 and 0.52 when s/d_e = 1.5, 2, 2.5 and 3, respectively. It was clear that a shift of the location of the minimum heat flux from the side jet towards the mid-point between the adjacent jets occurred as s/d_e was increased. For s/d_e = 3, three minimum values of local heat flux occurred at the stagnation point of the central jet, the inter-jet interference region and the stagnation point of the side jet (at y/s = 0, 0.52 and 1), respectively. When the jet-to-jet spacing increased, less significant influence between the adjacent jets was obtained. At the largest jet-to-jet spacing of s/d_e = 3, the thermal behavior of each flame jet in the array appeared to be an isolated jet. As shown in Fig. 3(g), a slight compression of the heat flux contours was found in the interacting side between the central and side jets, and the central jet was observed to have the thermal behavior of an isolated jet.

4.4. Effect of nozzle-to-plate distance (H/d_e)

The heat flux distributions along the y-axis of the impingement plate under different H/d_e ratios with large, moderate and small s/d_e ratios of 3, 2 and 1, are shown in Fig. 5(a)–(c), respectively. Another half of the figure (from 0 to 60 mm) has not been shown because of symmetry. There were three locations identified to illustrate the results, namely, the central jet's stagnation point, the

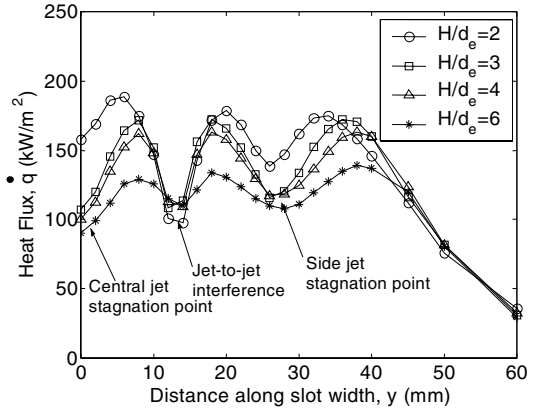

(a)

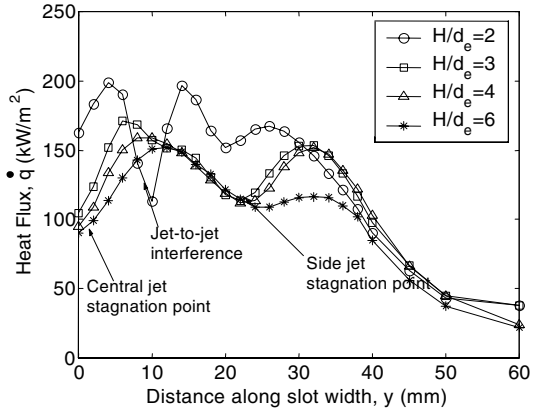

(b)

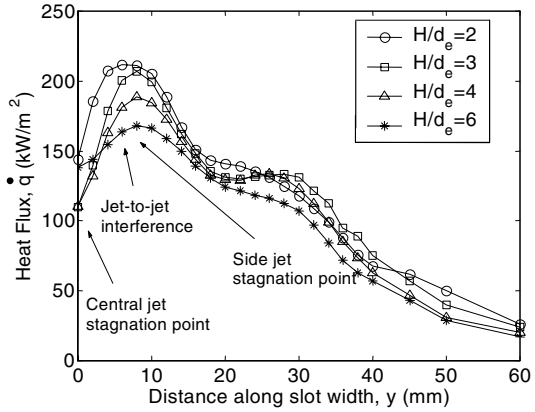

(c)

Fig. 5. Heat flux distribution along the slot width direction for different nozzle-to-plate distances (Re = 1000; ϕ = 1). (a) s/d_e = 3, and (b) s/d_e = 2, (c) s/d_e = 1.

jet-to-jet interference zone, and the side jet's stagnation point.

In Fig. 5(a), the heat transfer characteristics were quite similar for all H/d_e ratios. There was rather negligible influence on the heat transfer characteristics in the inter-jet interference zone and the wall jet region beyond the side jet's stagnation point at $y > 40$ mm. Three heat flux peaks were observed at different H/d_e ratios ranging from 2 to 6, two of which were located in the interacting zone between the central and side jets, and the third one was located in the non-interacting zone of the side jet. The lowest heat flux value was obtained between the two peaks in the inter-jet interference region, which was due to the collision of the adjacent flame jets to form a downward flow around the mid-point between them.

Thermal performance decreased when H/d_e was increased from 2 to 6, because the separation between the hottest conical luminous reaction zone and the impingement plate was increased. However, it should be noted that the length of the conical luminous reaction zone was not a constant but varied with Re, ϕ and configuration of the flame jet system. Thermal performance would also deteriorate when H/d_e became too small, such that the nozzle-to-plate distance was smaller than the length of the conical luminous reaction zone [27].

In Fig. 5(b), two heat flux peaks were found when $H/d_e \geqslant 3$, instead of three heat flux peaks as observed at $H/d_e = 2$. As s/d_e was reduced from 3 to 2, the outer flame layers of the adjacent flame jets started to interact with each other at sufficiently large nozzle-to-plate distance ($H/d_e \geqslant 3$). It led to a heat flux enhancement at the jet-to-jet interference region and pushed the cooler central core of the side jet to the non-interacting side. Thermal performance of the flame jets system decreased when the nozzle-to-plate distance was increased because of the same reason as mentioned previously.

When the s/d_e ratio was reduced to 1 as shown in Fig. 5(c), there was only one peak heat flux located at $y = 8.6$ mm for different H/d_e ratios ranging from 2 to 6. The peak heat flux was located around the stagnation point of the side jet. There was very strong interaction between the central and side jets when s/d_e was very small, such that the reaction zone and the outer flame layers of the side jet were displaced to the non-interacting side. The cooler central core of the central jet was clearly observed at $y = 0$ but that of the side jet, which was still observable at $s/d_e = 2$, no longer existed due to the interaction of the adjacent flame jets.

4.5. Area-averaged heat flux distribution

In order to seek the optimal jet-to-jet spacing with the best heat transfer performance, the area-averaged heat flux at various s/d_e ratios for the entire array, the central and side units of the jets were evaluated. The focus was concentrated to the stoichiometric flame (ϕ = 1) at laminar flow condition (Re = 1000) and small nozzle-to-plate distance ($H/d_e = 2$) due to the occurrence of high heat transfer at these conditions.

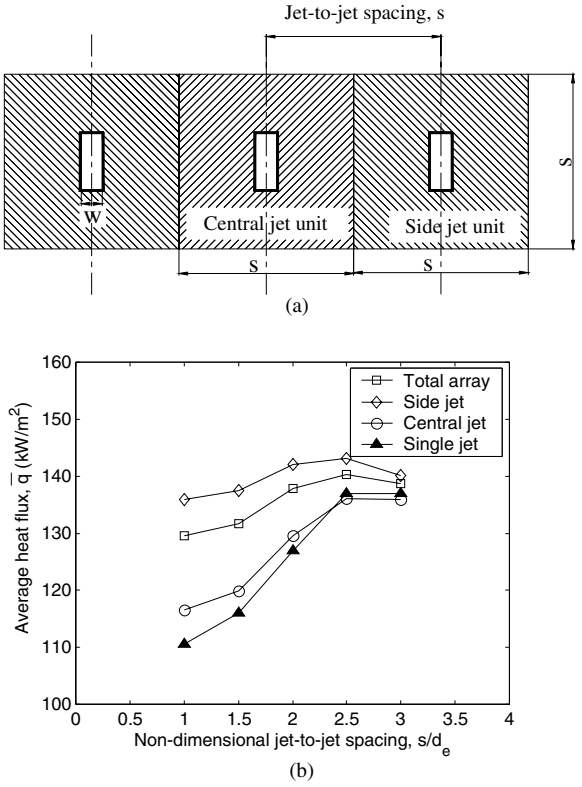

Fig. 6. Area-averaged heat flux. (a) Integrating areas for central and side jets and (b) variation with jet-to-jet spacing for single and multiple slot flame jets ($Re = 1000$; $\phi = 1$; $H/d_e = 2$).

The area-averaged heat flux distributions along the impingement plate surface were obtained by integrating the local heat flux values of the area under consideration as shown in Fig. 6(a), which was similar to that proposed by Dong et al. [26]. The area-averaged heat flux could be defined as:

$$\bar{q} = -\frac{\int\int_{(A)} \dot{q}\,\mathrm{d}A}{A} = \frac{\int_0^s \int_0^s \dot{q}(x,y)\,\mathrm{d}x\,\mathrm{d}y}{s^2} \quad (1)$$

In addition, in order to compare the area-averaged heat transfer performance between a single and an array of slot flame jets, experiments were performed at the same operating conditions for both single and multiple jet systems. The area-averaged heat flux of the central jet, side jet and all three jets of the jet array for various jet-to-jet spacings of 1, 1.5, 2, 2.5, and 3 are shown in Fig. 6(b). In addition, the area-averaged heat flux obtained from a singe slot flame jet has also been presented on the same figure for comparison purpose. It shows that the area-averaged heat flux of the entire jet array increased when the jet-to-jet spacing was increased from 1 to 2.5. However, further increase of the jet-to-jet spacing to 3 reduced the area-averaged heat flux slightly. The optimal jet-to-jet spacing corresponding to the highest area-averaged heat flux for the jet array under consideration was observed to be 2.5 at $Re = 1000$, $\phi = 1$ and $H/d_e = 2$. According to the Authors' previous studies [26,27,30,31], thermal characteristics of impinging jet varies with Reynolds number, equivalence ratio and nozzle-to-plate distance rather significantly. It is therefore very reasonable to expect that the optimal jet-to-jet spacing would be varied with Re, ϕ and H/d_e.

It was found that the area-averaged heat flux of the side jet was greater than that of the central jet. Such advantage was rather obvious at small s/d_e ratio and diminished as it was increased. At the small jet-to-jet spacing, the central jet experienced a strong interference with suppression from the two side jets, which acted as a large constraint for the central flame jet to develop. Thus, its flame length was relatively short when compared with that of the side jet as shown in Fig. 2. The heat flux received by the plate surface impinged by the central jet was reduced because the hottest conical luminous zone was relatively further away from the plate surface. In addition, part of the central flame jet was deflected towards the side jet at the small jet-to-jet spacing, causing a heat transfer enhancement of the side jet. However, it was observed that the three flame jets appeared as three isolated single flame jets when the jet-to-jet spacing was sufficiently large, which was evident by the area-averaged heat flux obtained at $s/d_e = 3$.

Comparing the area-averaged heat flux between a single slot flame jet and an array of triple slot flame jets, the side jet of the jet array was found to have higher heat flux than that of the central jet of the same array, as well as that of the single jet. It appeared that heat transfer enhancement had been obtained by using flame jets array especially at the small jet-to-jet spacing.

4.6. Comparison between multiple impinging round and slot flame jets

With the aim to compare the heat transfer performance of an array of impinging slot flame jets to that of the round jets, area-averaged heat flux of the triple slot flame jets obtained in the present study were compared with that suggested by Dong et al. [30], where the results were obtained under similar experimental conditions ($Re = 900$, $\phi = 1$ and $H/d = 2$). Fig. 7 shows the variation of area-averaged heat flux with non-dimensional jet-to-jet spacing for slot flame jet (s/w) and round jet (s/d). The s/w ratio was used in order for both systems to have same lateral spacing between adjacent jets.

It was observed that the maximum area-averaged heat transfer of the entire jet array occurred at s/w or $s/d = 5$, and the lowest heat transfer was obtained at s/w or $s/d = 2$, for both the slot and round jets. The slot flame jets appeared to have better heat transfer perfor-

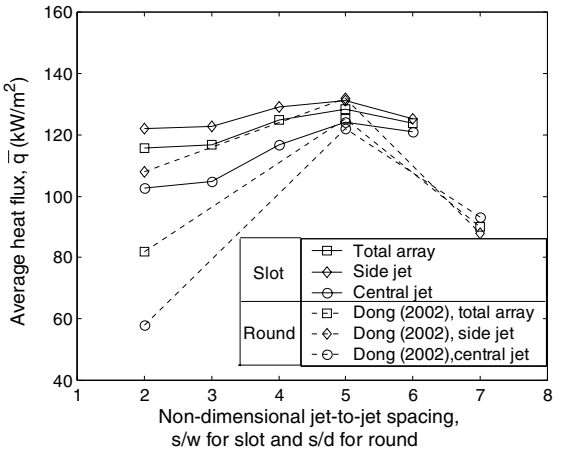

Fig. 7. Comparison of area-averaged heta flux of impinging multiple slot and round flame jets ($Re = 900$; $\phi = 1$; $H = 17.2$ mm).

mance than their counterparts. Besides, effect of the jet-to-jet spacing was more significant on the multiple round flame jets than the slot jets. It could be evident from the more rapid change in the area-averaged heat flux of the multiple round flame jets as the jet-to-jet spacing was varied. Compared with the slot flame jets, a greater discrepancy of area-averaged heat flux between the central and side jets was obtained with the round jets especially when the jet-to-jet spacing was small. Such significant discrepancy showed that the flow interference between adjacent jets was more pronounced for the round flame jets. It might be reasonable to suggest that the multiple slot flame jets were able to produce a higher and more uniform heat flux on the impingement plate.

5. Conclusions

The flame shapes and the heat fluxes on the impingement plate produced by a single slot flame jet and an array of triple slot flame jets, under different nozzle-to-plate distances and jet-to-jet spacings have been studied experimentally and the results are summarized as follows:

1. The between-jet interference decreased with increasing jet-to-jet spacing and nozzle-to-plate distance. Strong interference was obtained at the small jet-to-jet spacing of $s/d_e = 1$ and small nozzle-to-plate distance of $H/d_e = 2$, at which the central jet was suppressed to produce a shorter flame length while the side jets were deflected towards their free side. At the small jet-to-jet spacing, there was no minimum heat flux found in the inter-jet interacting zone; instead, a peak heat flux was obtained.
2. The heat flux received by the impingement plate was reduced when the nozzle-to-plate distance was increased from 2 to 6. It was due to the increased separation between the hottest conical luminous zone of the flame and the impingement plate as H/d_e was increased.
3. Location of the peak heat flux did not occur at the mid-point between adjacent jets but a location shifting towards the side jet, which was due to the strong inter-jet interference obtained there especially at the small jet-to-jet spacing. A peak heat flux was formed at the impinging zone between adjacent flame jets, while minimum heat fluxes were obtained at the stagnation points and the inter-jet interacting zone of the flame jets at $s/d_e = 2$ and 3.
4. The optimal jet-to-jet spacing corresponding to the highest area-averaged heat flux was found at $s/d_e = 2.5$ at $Re = 1000$, $\phi = 1$ and $H/d_e = 2$.
5. The resultant heat flux distributions of multiple slot flame jets were significantly different from those of a single slot jet. The area-averaged heat flux of the side jet of an array of slot flame jets was always higher than that of the central jet of the same array because of the suppression encountered by the central jet. However, the area-averaged heat flux of a single slot flame jet was close to that of the central jet of the multiple jets system when the jet-to-jet spacing was large ($s/d_e = 2.5$ and 3). In fact, the jets of an array of impinging slot flame jets appeared to be isolated single jets when the jet-to-jet spacing became sufficiently large ($s/d_e = 3$).
6. At small jet-to-jet spacing, the area-averaged heat flux of the multiple slot flame jets was higher than that of the round jets operating under the similar experimental conditions and arranging at the same geometric configuration. However, their area-averaged heat fluxes were close to each other as the jet-to-jet spacing became sufficiently large. As mentioned previously, the thermal behavior of each flame jet in the array appeared to be an isolated jet at $s/d_e = 3$.

Acknowledgement

The authors wish to thank The Hong Kong Polytechnic University for financial support of the present study.

References

[1] T.H. Van der Meer, Stagnation point heat transfer from turbulent low Reynolds number jets and flame jets, Expt. Therm. Fluid Sci. 4 (1991) 115–126.
[2] R.N. Koopman, E.M. Sparrow, Local and average transfer coefficients due to an impinging row of jets, Int. J. Heat Mass Transfer 19 (1976) 673–683.

[3] K.R. Saripalli, Laser doppler velocimeter measurements in 3-D impinging twin-jet fountain flows, Turbulent Shear Flows, vol. 5, Springer-Verlag, 1987, pp. 146–168.
[4] C. Carcasci, An experimental investigation on air impinging jets using visualization methods, Int. J. Therm. Sci. 38 (1999) 808–818.
[5] H. Martin, Heat transfer between impinging gas jets and solid surface, Adv. Heat Transfer 13 (1977) 1–60.
[6] R.J. Goldstein, J.F. Timmers, Visualization of heat transfer from arrays of impinging jets, Int. J. Heat Mass Transfer 25 (1982) 1857–1868.
[7] R. Gardon, J.C. Akfirat, Heat transfer characteristic of impinging two-dimensional jets, Trans. ASME, Series C, J. Heat Transfer 88 (1966) 101–107.
[8] A.M. Huber, R. Viskanta, Effect of jet–jet spacing on convective heat transfer to confined, impinging arrays of axisymmetric air jets, Int. J. Heat Mass Transfer 37 (1994) 2859–2869.
[9] N.R. Saad, A.S. Mujumdar, W.J.M. Douglas, Heat transfer under multiple turbulent slot jets impinging on a flat plate, Drying'80 1 (1980) 422–430.
[10] N.R. Saad, S. Polat, W.J.M. Douglas, Confined multiple impinging slot jets without crossflow effects, Int. J. Heat Fluid Flow 13 (1992) 2–14.
[11] J.M.M. Barata, D.F.G. Durao, M.V. Heitor, Impingement of single and twin turbulent jets through a crossflow, AIAA J. 29 (1991) 595–602.
[12] J.M.M. Barata, Fountain flows produced by multiple impinging jets in a crossflow, AIAA J. 34 (1996) 2523–2530.
[13] S.H. Seyedein, M. Hasan, A.S. Mujumdar, Laminar flow and heat transfer from multiple impinging slot jets with an inclined confinement surface, Int. J. Heat Mass Transfer 37 (1994) 1867–1875.
[14] C.E. Baukal, B. Gebhart, Heat transfer from oxygen-enhanced/natural gas flames impinging normal to a plane surface, Expt. Therm. Fluid Sci. 16 (1998) 247–259.
[15] M. Fairweather, J.K. Kilham, S. Nawaz, Stagnation point heat transfer from laminar high temperature methane flames, Int. J. Heat Fluid Flow 5 (1984) 21–27.
[16] A. Milson, N.A. Chigier, Studies of methane and methane-air flames impinging on a cold plate, Combust. Flame 21 (1973) 295–305.
[17] G.K. Hargrave, M. Fairweather, J.K. Kilham, Forced convective heat transfer from premixed flames. Part 1: Flame structure, Int. J. Heat Fluid Flow 8 (1987) 55–63.
[18] G.K. Hargrave, M. Fairweather, J.K. Kilham, Forced convective heat transfer from premixed flames. Part 2: Impingement heat transfer, Int. J. Heat Fluid Flow 8 (1987) 132–138.
[19] L.L. Dong, Studies of single and multiple impinging hydrocarbon flame jets, PhD Thesis, Department of Mechanical Engineering, The Hong Kong Polytechnic University, Hong Kong, 2002.
[20] M. Can, A.B. Etemoglu, A. Avci, Experimental study of convective heat transfer under arrays of impinging air jets from slots and circular holes, Heat Mass Transfer 38 (3) (2002) 251–259.
[21] J.W. Mohr, J. Seyed-Yagoobi, R.H. Page, Heat transfer from a pair of radial jet reattachment flames, J. Heat Transfer 119 (1997) 633–635.
[22] J. Wu, J. Seyed-Yagoobi, R.H. Page, Heat transfer and combustion characteristics of an array of radial jet reattachment flames, Combust. Flame 125 (2001) 955–964.
[23] C.E. Baukal, B. Gebhart, A review of flame impingement heat transfer studies. Part 1: Experimental conditions, Combust. Sci. Technol. 104 (1995) 339–357.
[24] R. Viskanta, Heat transfer to impinging isothermal gas and flame jets, Expt. Therm. Fluid Sci. 6 (1993) 111–134.
[25] R. Viskanta, Convective and radiative flame jet impingement heat transfer, in: The 9th International Symposium on Transport Phenomena in Thermal-Fluids Engineering, 1996, pp. 46–60.
[26] L.L. Dong, C.S. Cheung, C.W. Leung, Heat transfer from an impinging premixed butane/air slot flame jet, Int. J. Heat Mass Transfer 45 (2002) 979–992.
[27] L.C. Kwok, C.W. Leung, C.S. Cheung, Heat transfer characteristics of slot and round premixed impinging flame jets, Expt. Heat Transfer 16 (2003) 111–137.
[28] S.J. Kline, F.A. McClintock, Describing uncertainties in single-sample experiments, Mech. Eng. 75 (1953) 3–8.
[29] C.E. Baukal, B. Gebhart, Surface condition effects on flame impingement heat transfer, Expt. Therm. Fluid Sci. 15 (1997) 323–335.
[30] L.L. Dong, C.W. Leung, C.S. Cheung, Heat transfer of a row of three butane/air flame jets impinging on a flat plate, Int. J. Heat Mass Transfer 46 (2003) 113–125.
[31] L.L. Dong, C.W. Leung, C.S. Cheung, Heat transfer and wall pressure characteristics of a twin pre-mixed butane/air flame jets, Int. J. Heat Mass Transfer 47 (2004) 489–500.